**Supplementary Figures, Methods and References for**

# Direct imaging of single UvrD helicase dynamics on long single-stranded DNA

Kyung Suk Lee[1], Hamza Balci[2], Haifeng Jia[3], Timothy M. Lohman[3], Taekjip Ha[1,4*]

[1]Department of Physics, Center for Physics in Living Cells and Institute for Genomic Biology, University of Illinois, Urbana-Champaign, Urbana, IL 61801-2902, USA.

[2]Department of Physics, Kent State University, Kent, OH 44242, USA.

[3]Department of Biochemistry and Molecular Biophysics, Washington University School of Medicine, 660 South Euclid Avenue, Box 8231, St. Louis, MO 63110-1093, USA.

[4]Howard Hughes Medical Institute, University of Illinois, Urbana, IL 61801-2902, USA.

*Corresponding author: Taekjip Ha (tjha@illinois.edu)

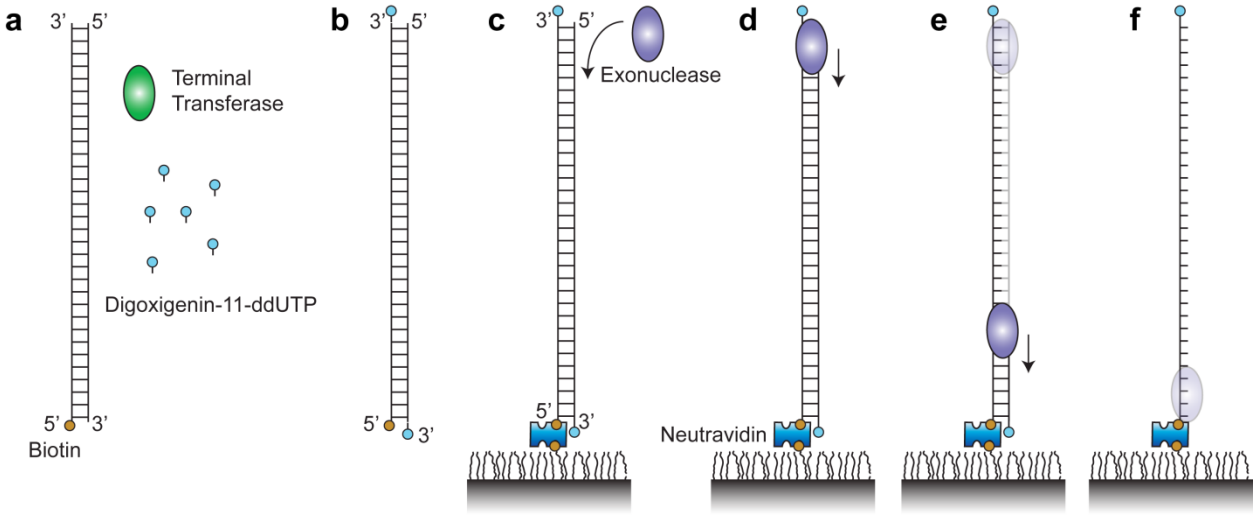


**Supplementary Figure S1.** Preparation of DNA constructs (a) Biotinylated 4957 bp dsDNA constructs are produced by PCR. (b) Terminal transferase is employed to label the 3'-ends of the constructs with digoxigenin. (c, d) The constructs are immobilized on the imaging surface, and T7 exonuclease is injected into the sample chamber to digest one strand away from the dsDNA constructs. (e) The end result is partial duplex DNA constructs with long 3'-ssDNA tails. (f) As the reaction time is increased, the ssDNA tail becomes longer, ultimately producing fully single-stranded constructs.

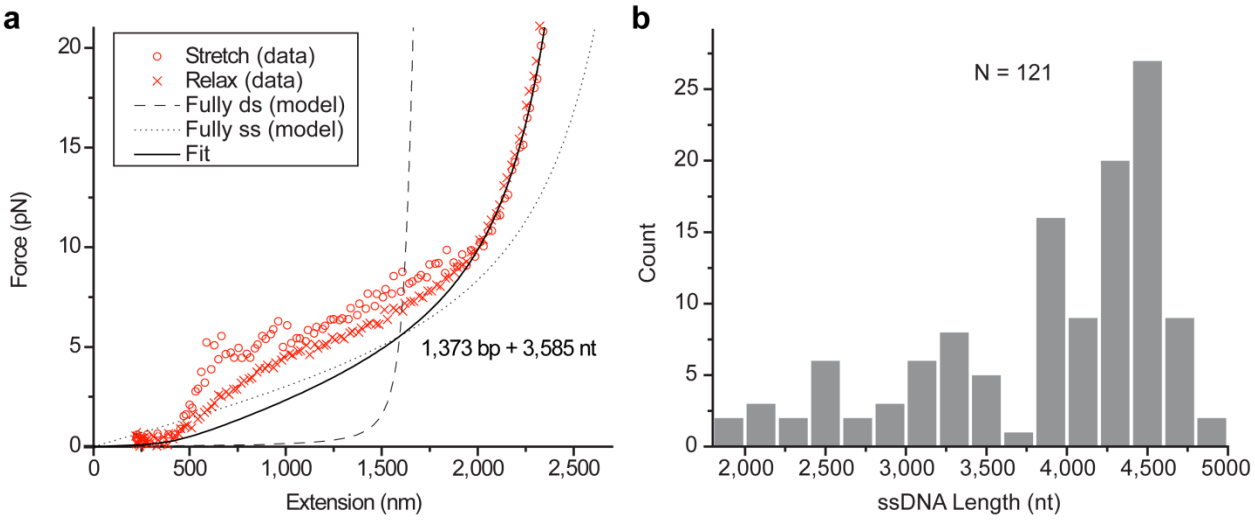


**Supplementary Figure S2.** Estimation of the length of the ssDNA segment within the DNA substrates (a) Force-extension curve of a DNA substrate shown with theoretical curves based on standard polymer models: the experimental data taken while the molecule is stretched (circle) and relaxed (cross) are in red; the theoretical curves for fully dsDNA (4,958 bp, dashed line), fully ssDNA (4,958 nt, dotted line) in black, and the fitting result (1,373 bp + 3,585 nt). Unzipping of secondary structures is observed while the molecule is stretched, so only the data points at very low forces, where the molecule behaves like a DNA with only the dsDNA segment, and at forces above ~10 pN, where all the secondary structures are removed, are used for fitting. This molecule has ~1,400 bp (dsDNA) and ~3,600 nt (ssDNA). (b) The distribution of ssDNA lengths within the DNA constructs. After 30 min of T7 exonuclease digestion, more than half of the DNA constructs possess a ssDNA segment longer than 4,000 nt.

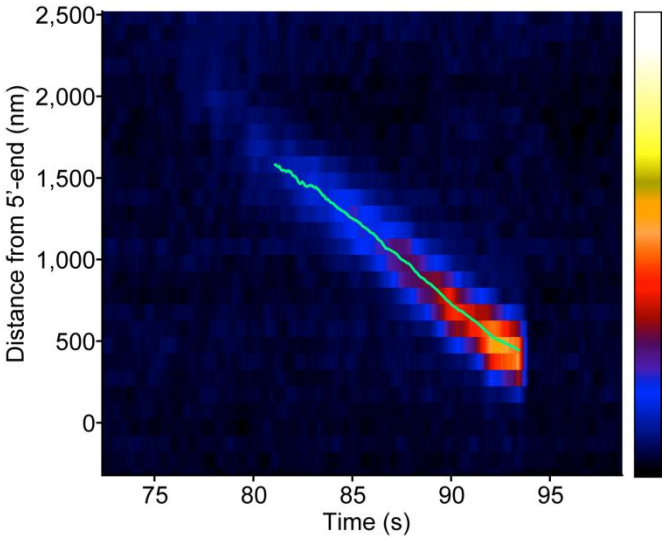


**Supplementary Figure S3.** A kymogram of a translocating UvrD. The position trajectory (light green) obtained from 2D Gaussian fitting of fluorescence images is overlaid on top.

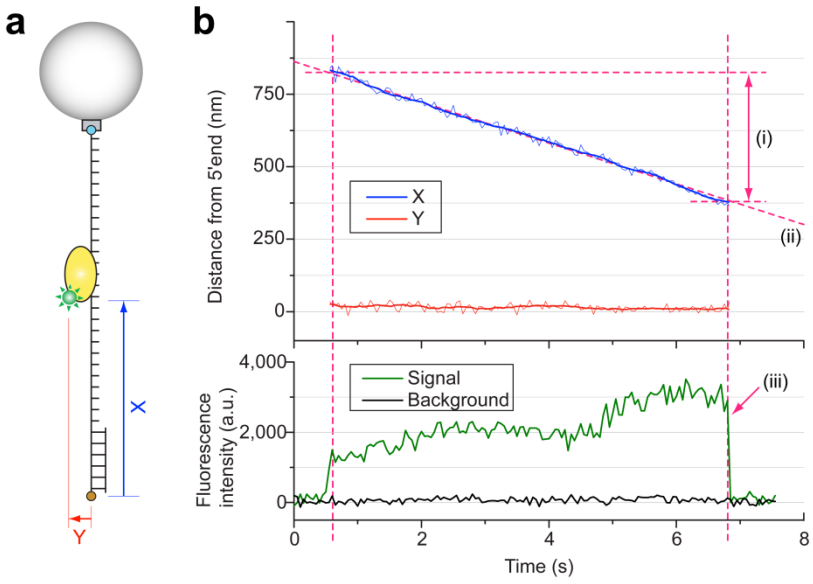


**Supplementary Figure S4.** Analysis of translocation trajectories (a) The 5'-end of the DNA substrate (brown circle) is chosen as the origin. The X axis (blue) is along the DNA toward the 3'-end (light blue circle), while the Y axis (red) is in the direction perpendicular to the X axis. (b) The position and fluorescence intensity trajectories of a fluorophore-labeled UvrD were obtained from 2D Gaussian fitting of the fluorescence images. In the top graph, the blue and red lines represent the positions along the X and Y axes, respectively. The thin lines are the fitting results from a single frame at the frame rate of 20 Hz, while the thick lines are those of the moving average of 10 frames. The bottom graph shows the fluorescence intensity trajectories from the dye (green) and the background (black). Binding and dissociation of a protein can be monitored by the sudden jump and drop in the fluorescence intensity (magenta dashed line). (i) the distance which this protein translocated (ii) the position trajectory is fit to a straight line to determine the speed of translocation (iii) the number of photo-bleaching steps gives information on the number (stoichiometry) of proteins on the DNA. The fluorescence intensity gradually increases as the protein approaches the surface due to the exponentially decaying excitation field. There is a wiggle in the fluorescence intensity because the illumination is not perfectly uniform throughout the entire imaging area due to interference of the coherent light used.

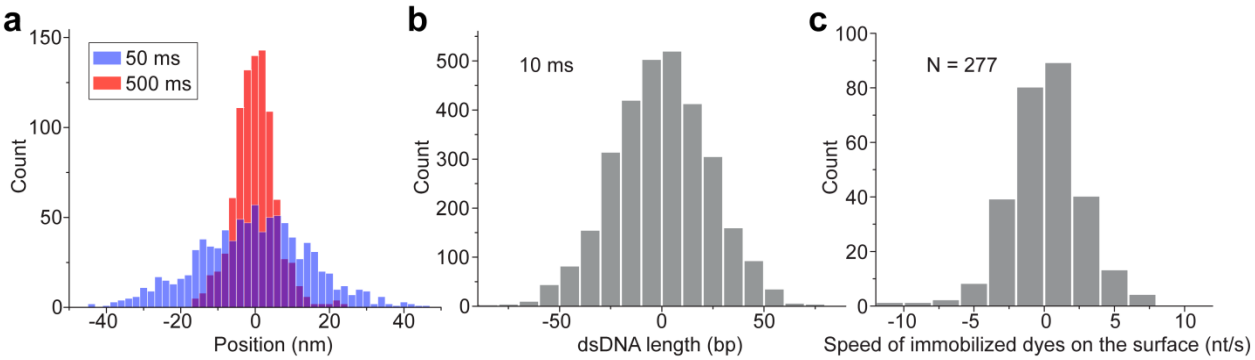


**Supplementary Figure S5.** Measurement errors. (a) Errors in the position measurement estimated by 2D Gaussian fitting. The position of a stalled UvrD at a junction determined by 2D Gaussian fitting with 10 frame averaging (red) and without averaging (blue) is shown. The standard deviation of the distribution is the estimate of the spatial precision and it is 6 nm at a time resolution of 500 ms (red) and 15 nm at 50 ms (blue). The actual spatial precision should be better than this because the position of the stalled protein includes the drift of the sample, the fluctuation of the DNA tether, and the movement of protein itself. (b) Errors in the unwinding measurement. The change in the length of the dsDNA segment was determined by the change in the applied tension. Thus, we calculated the change in the length of the dsDNA segment for the data points collected at a time resolution of 10 ms for a 20 s interval in which the tension was stable. Since the tension was stable, the change in the length of the dsDNA segment in this interval should be zero. Indeed, the mean of the distribution was zero, but it has a standard deviation of 23 bp, which is the estimate for the error in the unwinding measurement. (c) Errors in the translocation rate measurement. The positions of dyes immobilized on the surface were monitored and the speed was calculated in the same way as it was measured for the translocation of UvrD molecules. The distribution of rates is the combination of both the drift of the surface and the noise in the speed measurement. Both were negligible as the mean and the standard deviation of the distribution is 0.13 nt/s and 2.57 nt/s, respectively.

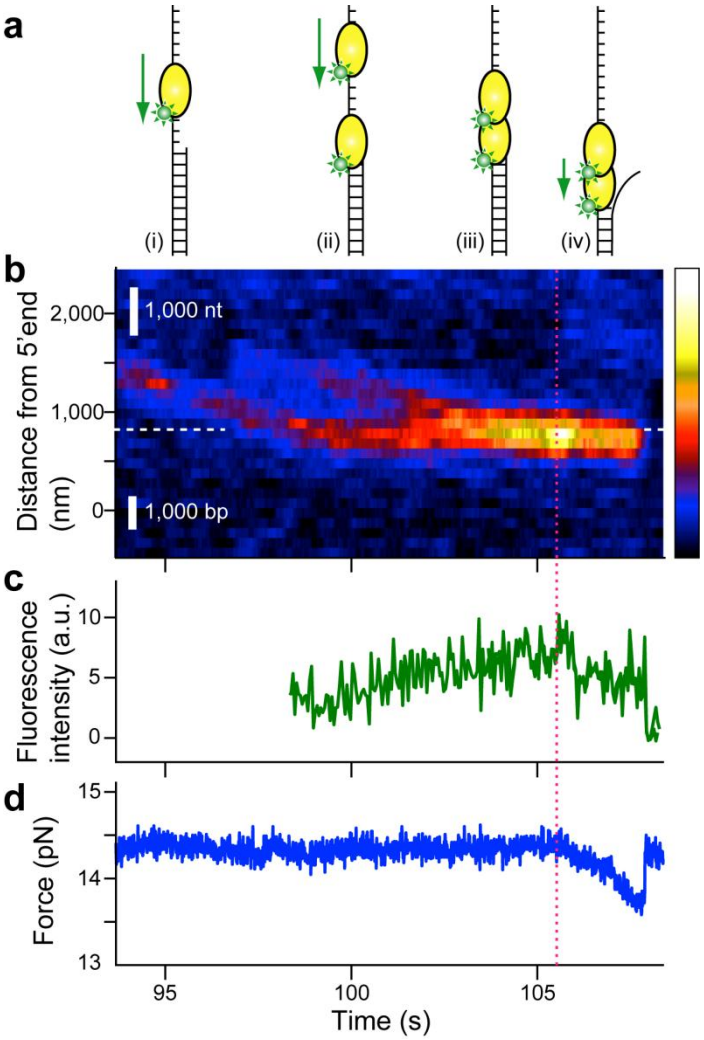


**Supplementary Figure S6.** Two translocating UvrD molecules join at the ssDNA/dsDNA junction to initiate unwinding. (a) Schematic of this unwinding event. (i) The first UvrD translocates down to the junction. (ii) The first one stalls at the junction, while the second UvrD binds and translocates. (iii) Two UvrD molecules form an active dimeric helicase complex. (iv) The helicase unwinds dsDNA. (b) The kymograph of this event. The white arrow points to the estimated location of the ssDNA/dsDNA junction. Two UvrD molecules merge at the junction. (c) The fluorescence intensity trajectory. As the second UvrD approaches the junction, the intensity gradually increases. After initiation of unwinding, one fluorophore photobleaches. (d) The plot of force vs. time shows that tension on the DNA starts to decrease at the time point indicated by the magenta dotted line.

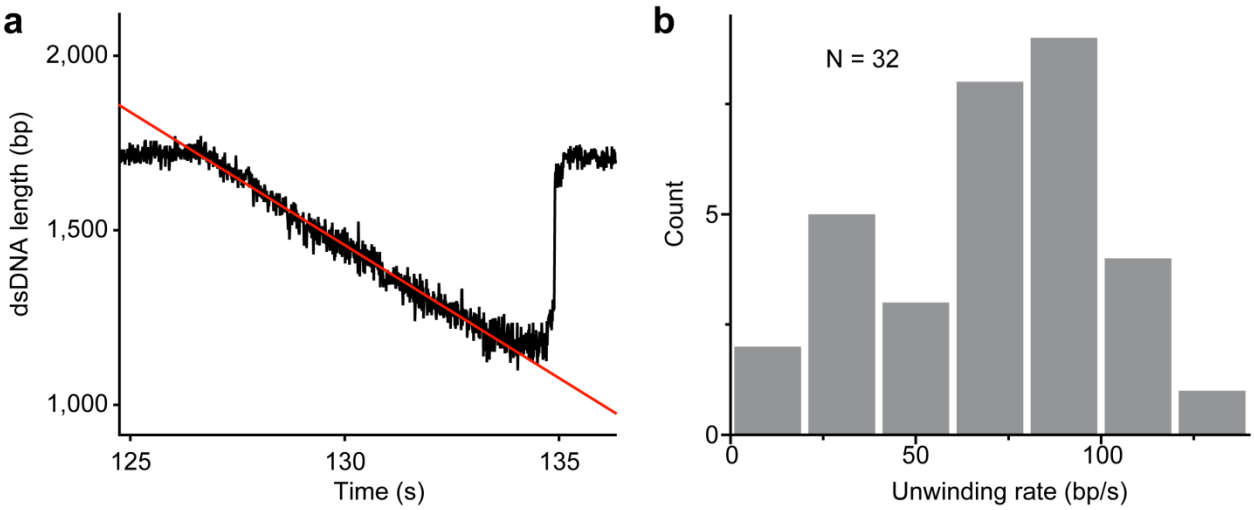


**Supplementary Figure S7.** Unwinding rate of UvrD. (a) How the unwinding rate is determined. The time course of the change in the length of the dsDNA segment is calculated from time course of DNA tension and end to end distance of the DNA, using the XWLC and XFJC models. The intervals that show unwinding (decrease of dsDNA length) were fit to a straight line (red), to obtain the rate. (b) The distribution of unwinding rates from 32 events. The mean and the standard deviation (SD) are 70 bp/s and 31 bp/s, respectively.

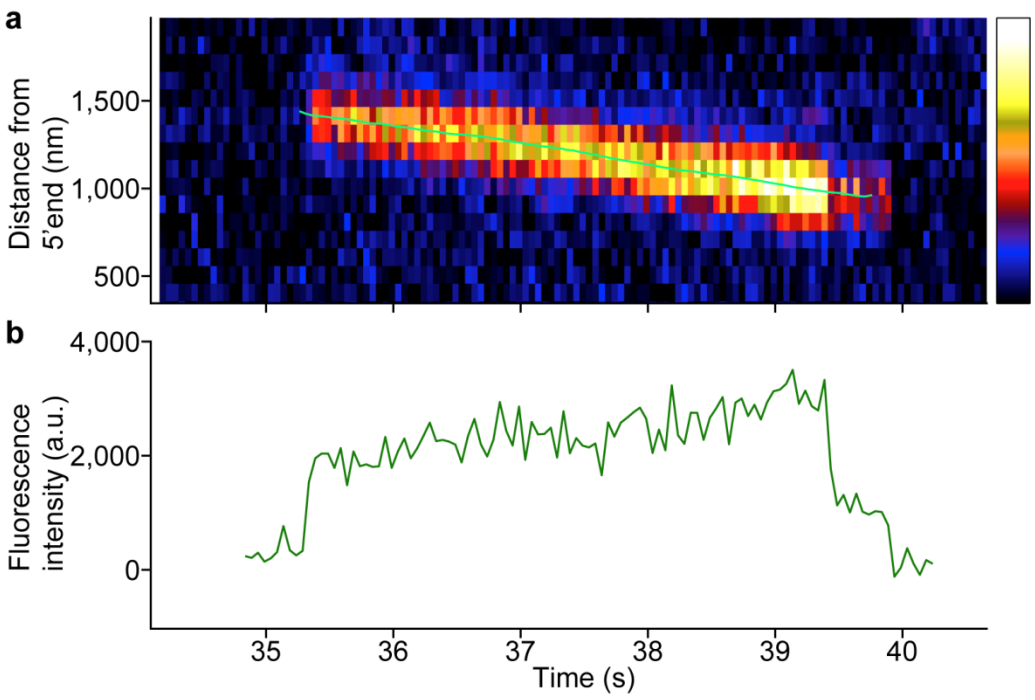


**Supplementary Figure S8.** Binding of dimeric UvrD. (a) At least two UvrD monomers bind to DNA, at the same time, within our measurement error (50ms). Since it is very unlikely that two independent monomers bind to the same position of ssDNA at the same time, this event should be binding of dimeric species of UvrD. They translocate at a rate of 225 nt/s, which is comparable to that of a monomer. At 39.5 s, one fluorophore disappears either by photobleaching or dissociation, but the position of the UvrD molecules obtained from a 2D Gaussian fit (light green) does not show a significant difference before and after the loss of the fluorophore. The speed of the remaining fluorophore is 200 nt/s. Unlike the other kymograms, a moving average is not taken in order to show the fluorescence intensity changes more sharply. (b) The intensity trajectory of this molecule displays a clear one step intensity jump followed by a two-step decrease.

## Supplementary Methods

### *Dual fluorescent-force instrument design*

The instrument used in this study is an objective-type TIRF microscope with a single optical trap. However, to merge the two single-molecule techniques without impairing the capabilities of either technique, we made certain adjustments. One of the challenges in combining the two techniques is that the fluorescent lifetime of fluorophores is greatly reduced by the optical trap [61], presumably due to the massive photon flux from the trap. In addition, a section of DNA adjacent to the trap remains out of the evanescent field of fluorescence illumination and cannot be imaged. To minimize the invisible portion of a DNA tether, the height of the trap must be adjusted to be as close to the surface as possible. For the same reason, it is advantageous to use longer DNA, which mitigates the enhanced photobleaching by separating most of the DNA by a large distance from the trap. However, this needs to be considered in conjunction with the fact that the resolution for detecting changes in tether extension decreases with increasing tether length, and the requirement to fit the entire DNA within the CCD camera screen.

### *Instrument calibration*

A sample of Cy3-labeled DNA oligonucleotides and beads immobilized on the surface is imaged by bright-field microscopy at various axial positions, which are obtained by displacing the sample with a piezoelectric stage. The defocused images of beads are used to calibrate the relation between the defocusing radius of the beads in bright-field images and the axial displacement of the beads from the fluorescence focus, which is determined by monitoring the fluorescence of the Cy3 fluorophore [62]. Then, using, another sample of Cy3-labeled DNA oligonucleotides immobilized on the surface with free beads, a bright-field image of a trapped bead at the fluorescence focus is recorded to find the defocusing radius of a trapped bead and to determine the height of the optical trap. To map the quadrant photodiode detector (QPD) response to the lateral position of a trapped bead, a DNA construct is stretched while the bead is

imaged by bright-field illumination. For each frame, we get the lateral displacement of the trapped beads in the bright-field images and the voltage signal from the QPD. With this relation, a calibration curve is created. Finally, to determine the stiffness of the trap, we use the power spectrum method [63]. The corner frequency is determined by fitting the power spectrum of the thermal motion of a trapped bead to a Lorentzian function. The drag coefficient is theoretically estimated using Faxen's law [63] or experimentally determined by measuring the power spectrum of a trapped bead while the sample is driven sinusoidally using the piezo stage. The response to the sinusoidal motion in the power spectrum can be used to determine the drag coefficient experimentally [64].

### *Surface preparation*

A coverglass of white borosilicate (VWR) and a quartz slide are coated with a layer of polyethyleneglycol (PEG) to passivate the surface and inhibit nonspecific adsorption of proteins, following a common protocol for preparing the PEGylated surface [65] A subpopulation of PEG molecules is biotinylated, so that biotinylated DNA constructs can be immobilized on the surface through biotin-neutravidin-biotin bonds.

### *Determination of DNA substrate location on camera screen*

Since DNA is invisible in our fluorescence images, we locate a DNA substrate in the following way. Prior to the experiment, the position of a fluorescent bead immobilized on the surface is tracked while scanning the piezo stage in the X and Y axis, to create a mapping between the piezo stage and the camera screen. After trapping a bead tethered by a DNA substrate on the surface, the applied tension to the DNA tether is measured as the piezo stage is moved back and forth along the X axis to find the origin of symmetry. The same steps are repeated for the Y axis to find the origin in the Y axis. The origin corresponds to where the DNA is tethered on the surface. When the stage is at the origin of the stretching curves, a trapped bead that is at the center of the trap should be on top of the tethering point, i.e. the 5'-end of the tracking strand. At the origin, we image the trapped bead with bright-field illumination, and fit the image to a 2D

Gaussian to mark the lateral position of the trapped bead, which should correspond to the position of the 5'-end. This procedure is done for every bead before starting the fluorescence imaging. As the stage is moved to stretch the DNA, the position of the 5'-end is tracked on the camera screen using the aforementioned mapping. This locates the position of the 5'-end and the position of a trapped bead on which the 3'-end of the tracking strand is attached. The DNA substrate lies between these two points.

### *Generation of a Kymogram*

We smooth a movie by taking a moving average of 10 frames. For each frame of the 'smoothed' movie, the intensity of pixels near the line segment where a DNA construct lies is analyzed. For each pixel on the line, we take the mean of the intensity of the pixel and the 2 neighboring pixels across the line to generate a strip with a 1 pixel width for the frame. This is repeated for all frames and the strip for each frame is put together to generate an image as wide as the number of frames.

## Supplementary References


61. van Dijk, M.A., Kapitein, L.C., van Mameren, J., Schmidt, C.F. & Peterman, E.J.G. Combining Optical Trapping and Single-Molecule Fluorescence Spectroscopy: Enhanced Photobleaching of Fluorophores. *The Journal of Physical Chemistry B* **108**, 6479-6484 (2004).
62. Toprak, E., Balci, H., Blehm, B.H. & Selvin, P.R. Three-Dimensional Particle Tracking via Bifocal Imaging. *Nano Letters* **7**, 2043-2045 (2007).
63. Neuman, K.C. & Block, S.M. Optical trapping. *Review of Scientific Instruments* **75**, 2787-2809 (2004).
64. Tolic-Norrelykke, S.F. et al. Calibration of optical tweezers with positional detection in the back focal plane. *Review of Scientific Instruments* **77**, 103101-11 (2006).
65. Selvin, P. & Ha, T. *Single-Molecule Techniques: A Laboratory Manual*, (Cold Spring Harbor Laboratory Press, 2008).